THE JOURNAL OF PHYSICAL CHEMISTRY A

Article

pubs.acs.org/JPCA

Spectral and Kinetic Study of 3-Methylquinoxalin-2-ones Photoreduced by Amino Acids: *N*-Phenylglycine Radical Chain Reactions and *N*-Acetyltryptophan Decarboxylation

Julio R. De la Fuente,*[,†] Álvaro Cañete,[‡] Natalia Carathanassis,[†] Luan Bernazar,[†] Claudio Saitz, and Dafne Díaz-Hernández[†]

[†]Departamento de Química Orgánica y Fisicoquímica, Facultad de Ciencias Químicas y Farmacéuticas, Universidad de Chile, Casilla 233, Santiago 1, 6640750 Chile

[‡]Departamento de Química Orgánica, Facultad de Química, Pontificia Universidad Católica de Chile, Casilla 306, Correo 22, Santiago, Chile

Supporting Information

ABSTRACT: Transient intermediates were identified in the photoreduction of 3-methylquinoxalin-2-one derivatives by *N*-phenylglycine, NPG, and *N*-acetyltryptophan, NAT. For both reductants it can be postulated a sequence of reaction comprising first a photoinduced single electron transfer followed by a proton transfer from the radical cation of the electron donor to the radical anion of the 3-methylquinoxalin-2-one giving rise to the reported products. The effect of the concentrations of NPG and the quinoxalin-2-one on the rate of photoconsumption of this last were quantified, and the lifetimes of the possible intermediates estimated. In the photoreduction by NAT, processes leading to the decarboxylation of NAT and radical adduct product compete with the expected SET from the indoyl N to the excited triplet of quinoxalin-2-ones as revealed by the detection of the deprotonated *N*-acetyltryptophan radical [NAT-H]$^{\bullet}$. This radical is formed almost instantly after the laser pulse and has a secondary delayed growth via a delayed proton transfer from the indoyl radical cation NAT$^{\bullet+}$ to the quinoxalin-2-one radical anions. The decarboxylation of NAT that mimics C-terminus tryptophan in proteins is biologically relevant because might cause damages at cellular and the whole organism level. As far as we know this is the first report of a radical decarboxylation of *N*-acetyltryptophan leading to photoproducts.

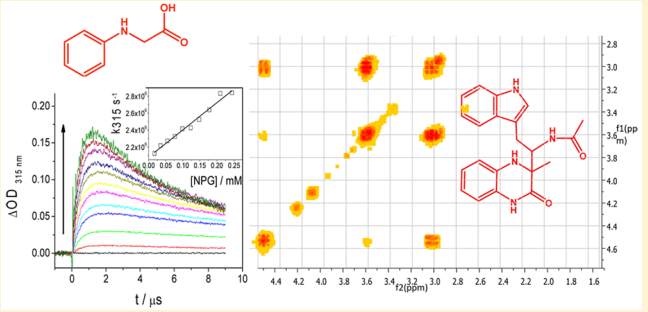

INTRODUCTION

Quinoxalin-2-ones derivatives have received considerable attention in the last decades due mainly to their various pharmacological properties. These compounds exhibit bacteriostatic, virostatic and anticarcinogenic effects and even, some derivatives are active against HIV reverse transcriptase.[1−11] However, even with all of the biological interest in this class of compounds, there are relatively few references concerning the derived radicals generated by either electrochemical[12] or photochemical processes.[13] The oxidative processes by $^{\bullet}$OH and $^{\bullet}N_3$ radicals of quinoxalin-2-one and 3-methylquinoxalin-2-one were studied by pulse radiolysis in water at pH 7,[14] and more recently the pulse radiolysis transient spectra of the radical anions and the protonated radical ions, in water with absorptions at 390 nm and a prototropic equilibrium between the radical anions and the protonated radical ions (pK_a > 13.5) have been reported.[15] Even so, there are some references reporting the photoreaction products of quinoxalin-2-ones derivatives in different systems.[16−24] Recently we reported the unexpected generation of imidazoquinoxalinone annulation products obtained in the photoinitiated reduction of substituted 3-methyl-1*H*-quinoxalin-2-ones with *N*-phenylglycine, NPG.[13] The formation of the imidazoquinoxalinone products requires of the decarboxylation of the NPG radical cation, NPG$^{\bullet+}$ that is generated by a single electron transfer, SET, to the 3-methyl-1*H*-quinoxalin-2-one excited triplet,[3]MQ. These NPG decarboxylations, which are photoinitiated by SET between heterocyclic and polycyclic aromatic compounds, have been widely reported.[25−29] Similar processes, sensitized or catalyzed by carbonyl compounds, have also been reported.[30−33] The decarboxylations of NPG radical cations, which are generated by SET, occur with rates ranging between 10^6−10^8 s^{-1}, giving rise to the recognized highly reducing α-amino-alkyl radical PhNHCH$_2^{\bullet}$.[34−36] This last have easy to follow reported absorptions at 400 and 307 nm, as was shown experimentally and by quantum mechanics calculations.[37] Moreover, a fast decarboxylation of the radical cation of *N*-phenylglycine, NPG$^{\bullet+}$, should prevent a back electron transfer in the initial

Received: February 3, 2016
Revised: April 11, 2016
Published: April 15, 2016

DOI: 10.1021/acs.jpca.6b01141
J. Phys. Chem. A 2016, 120, 2797−2807

radical-ion pair. The radical cation, $NPG^{\bullet+}$ has been well characterized by pulse radiolysis experiments in water,[38] showing an absorption with maxima at 460 nm at pH = 6. At basic pH, this species evolves rapidly into the deprotonated radical cation, $[NPG\text{-}H]^{\bullet}$, absorbing at 420 nm. The authors also reported a reduction potential $E°(NPG^{\bullet+}/NPG)$ = 0.89 V v/s normal hydrogen electrode, NHE, at pH = 6.[38] Therefore, by flash photolysis, among the absorption of quinoxalin-2-one radical anion, $MQ^{\bullet-}$, expected from a SET from NPG, one can expect to observe an early absorption from $NPG^{\bullet+}$ at 460 nm, followed by absorptions at 400 and 307 nm due to the α-aminoalkyl radical $PhNHCH_2^{\bullet}$ generated by decarboxylation of $NPG^{\bullet+}$. These absorptions should be accompanied by those corresponding to radicals derived from quinoxalin-2-ones. In our previous work,[13] we reported the unexpected formation of imidazoquinoxalin-2-ones and radical chain reactions that explain the observed large quinoxalin-2-ones photoconsumptions quantum yields. In the present paper we report a flash-photolysis study of seven 3-methyl-1*H*-quinoxalin-2-ones in the presence of *N*-phenylglycine, NPG, and *N*-acetyltryptophan, NAT. This study shows clear spectroscopic and kinetic evidence of radical chain reactions in the presence of NPG. It also presents the spectroscopic characterization of the transient species generated in the presence of NAT by the 3-methyl-1*H*-quinoxalin-2-ones. The reduction potential for NAT, $E°(NAT^{\bullet+}/NAT)$, should not be so different from those reported for tryptophan and some methylindole derivatives, ranging between 1.23 and 0.93 V.[39−41] These values are in the same $E°$ range of amines that we previously used to photoreduce 3-phenylquinoxalin-2-one derivatives.[16,17] Therefore, it is reasonable to expect a SET from NAT to the substituted quinoxalin-2-one. For NAT derived radicals, transient absorptions are expected near 560 nm for the radical cation $NAT^{\bullet+}$ and close to 510 nm for the deprotonated neutral radical $NAT\text{-}H^{\bullet}$, similar to those reported for tryptophan radicals.[40,42−47]

EXPERIMENTAL SECTION

Materials. Acetonitrile Merck, HPLC grade, was used as received. *N*-Phenylglycine, Aldrich 97%, was crystallized twice from water before use, *N*-acetyl-L-tryptophan Sigma-Aldrich >99% was used as received, and 1,4-diazabicyclo[2.2.2]octane, DABCO, Aldrich 98%, was purified by sublimation before use. **Photoconsumption quantum yields (Φ_C)** were evaluated from the initial photoconsumption rates, R_0, that were measured at the maximum of the lower energy absorption band of the respective substrates and corrected by the initial sample absorption at 366 nm, A_{366}, against Aberchrome540,[48] taking Φ_{Aber} = 0.2 and ε_{Aber} at 494 nm as 8200 M^{-1} cm^{-1}. The expression used for quantum yield was $\Phi_C = (R_0/\varepsilon_{\lambda_{max}} \times \Phi_{Aber})/[R_{Aber}/\varepsilon_{Aber} \times (1-10^{-A_{366}})]$, where $\varepsilon_{\lambda_{max}}$ is the absorption coefficient of quinoxalin-2-one at the wavelength maximum, R_0 is the rate of disappearance of absorbance at λ_{max}, and R_{Aber} is the rate of the appearance of aberchrome absorption at 494 nm. All these experiments were made with 3 mL acetonitrile solutions of 7-methoxy, 7-trifluorometyl, and the unsubstituted 3-methyl-1*H*-quinoxalin-2-one, approximately 0.1 mM at absorbances between 0.9 and 1.5 and with [NAT] > 1 mM.

Laser flash photolysis experiments were performed on our modernized instrument described previously.[13] The flash photolysis setup is now provided with a Continuum Surelite I 10 Hz Q-switched Nd:YAG laser with the second and third harmonic generators. The signals are captured by a Hamamatsu 928 photomultiplier into a WaveSurfer 600 MHz LeCroy oscilloscope. Software written in National Instrument LabViews 8.0 controls the laser, monochromator, and shutters. The captured data are fed into a program, written in Igor Pro 6.3, for treatment and display. The system is provided with a peristaltic pump and a 0.5 mL flow cell to ensure the continuous renovation of solutions. Optimal results were obtained with solutions with absorbances between 0.4 and 0.6 at the 355 nm excitation wavelength. The laser power impinging the cell was attenuated to typically ≈10 mJ/pulse by using glass plates. Quenching experiments were typically made with solutions (3 mL) of substrates bubbled with Ar for 20 min in 10 mm square quartz cells sealed with a septum. After purging, aliquots of quenchers were added, and the lifetimes τ at defined wavelengths were measured. Quenching constants were obtained from slopes of Stern−Volmer type plots of $1/\tau$ vs [quencher] which were linear with r > 0.98 in all of the experiments.

Transient spectra in the presence of DABCO, NPG, and NAT were obtained with Ar bubbled 250 mL acetonitrile solutions containing 0.1 mM of the quinoxalin-2-one and variable amounts of the quenchers. These solutions were monitored in a 10 mm light path 0.5 mL flow cell at a flow rate of ≈1 mL/min taking an average of five laser shots for each monitored wavelengths at each quencher concentration used. Ar bubbling was performed during the whole experiments.

Preparative Photolyses. Preparative photolyses were done with derivatives **1d** in solutions containing an excess of NAT (10 equiv) and 40 mg (1.8 mmol) of **1d** in HPLC quality acetonitrile that had been bubbled with N_2 for 1 h. The solution was photolyzed, at room temperature, for 24 h under continuous N_2 bubbling and stirring. The light source used was a 150 W Black Ray UV lamp equipped with a 366 nm filter at 10 cm. The postirradiation reaction mixture was filtered, and the filtrate was evaporated to dryness. Finally, the photoproducts were separated by flash column chromatography on silica gel using CH_2Cl_2/ethyl acetate 1:1 as the eluent. The fractions of interest were dried out and dissolved in $CDCl_3$ for NMR and mass spectroscopy.

HRMS-ESI were done by using a Thermo ScientificExactive Plus Orbitrap spectrometer with a constant nebulizer temperature of 250 °C. The experiments were carried out in the positive ion mode, with a scan range of m/z 100−600 with a resolution of 140000. The samples were infused directly into the ESI source via a syringe pump at flow rates of 5 μL min^{-1}.

NMR Spectroscopy. ^1H NMR, COSY, HMBC, HMQC, and ^{13}C NMR DEPT 135° were done in a Bruker Advance DRX-400, 400 MHz spectrometer, using tetramethylsilane as the internal standard. Due to the low concentration of the samples, the experiments lasted for several hours.

Photoproduct of 3-Methylquinoxalin-2-one and NAT NMR Description. $C_{21}H_{22}N_4O_2$: ^1H NMR (400 MHz, $CDCl_3$) δ 1.47 (s, 3H), 1.88 (s, 3H), 3.02 (dd, J = 15.4, 10.4 Hz, 1H), 3.62 (dd, J = 15.4, 2.7 Hz, 1H), 4.24 (s, 1H), 4.54 (dt, J = 10.4, 2.7 Hz, 1H), 6.64 (d, J = 7 Hz, 1H), 6.71−6.76 (m, 2H), 6.83 (d, J = 10.4 Hz, 1H), 6.88−6.92 (m, 1H), 7.02−7.06 (m, 2H), 7.10−7.14 (m, 1H), 7.26−7.32 (m, 1H), 7.54 (d, J = 7 Hz, 1H), 8.11 (s, 1H), 8.33 (s, 1H).

^{13}C NMR (125 MHz, $CDCl_3$): δ 23.1, 23.5, 25.9, 56.5, 61.5, 111.2, 112.6, 114.3, 115.1, 118.6, 119.0, 119.2, 121.8, 121.9, 123.7, 124.4, 127.9, 132.7, 136.2, 170.3, 170.7.

DOI: 10.1021/acs.jpca.6b01141
J. Phys. Chem. A 2016, 120, 2797−2807

HRMS for $C_{21}H_{23}N_4O_2$ $[M + H]^+$ Calcd: 363.1821. Found: 363.1808.

HRMS for NAT dimer $C_{14}H_{28}N_4O_2$, Calcd: 404.2212. Found 404.2550.

RESULTS AND DISCUSSION

In our previous results[13] on the steady-state photolysis of the 7-substituted quinoxalin-2-ones in the presence of NPG, the photoconsumption quantum yields showed a strong dependency on the electron withdrawing or donating properties of the substituents. In light of these experiments, we decided to check whether we could observe the same behavior in photoreactions with NAT. For this reason, in the photoconsumption study, we choose some of the quinoxalin-2-ones of Scheme 1, which permitted sweeping the electrophilic substituent parameter σ^+ from −0.778 to +0.612. We expected to observe the maximal effect by using quinoxalin-2-ones **1a**, **1d**, and **1f**.

Scheme 1. 3-Methyl-1*H*-quinoxalin-2-ones

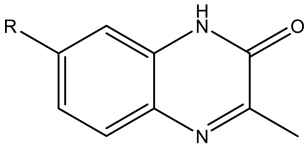

1

R
a = CH_3O
b = CH_3
c = F
d = H
e = Br
f = CF_3
g = CN

These derivatives did not show significant spectral changes when photolyzed in aerated acetonitrile irrespective of the NAT presence. However, in argon-saturated solutions significant spectral changes at short times were observed, suggesting that the photoreaction proceeded mainly, if not exclusively, from their triplet excited state. During the photolysis at least one isosbestic point was be observed, meaning that only one product or a stoichiometric mixture of products was formed. For the studied derivatives, **1a**, **1d**, and **1f**, the initial rates, R_0, depended on the [NAT]. These initial rates reached plateau values at relatively high molar ratios that were selected to measure the photoconsumption quantum yields, Φ_c. An example of this photoreaction for 7-methoxy-3-methylquinoxalin-2-one, **1a**, is shown in Figure 1. In the upper inset of Figure 1, a kinetic profile that was monitored at the maximum of lowest energy absorption band, λ = 361 nm, is shown. In the lower inset of Figure 1, the initial rates measured at various [NAT] are shown. The Φ_c results, which were measured in their respective plateau regions, showed slightly different values for each of the derivatives, giving values of Φ_c = 0.61, 0.72, and 0.45 for the CH_3O- (**1a**), H- (**1d**), and CF_3-substituted (**1f**) 3-methylquinoxalin-2-ones, respectively. These results preclude a dependency of Φ_c on the Hammetts' substituent parameter σ^+ and a possible radical chain reaction between the quinoxalin-2-ones and NAT.

Photoreduction Products of 3-Methylquinoxalin-2-one and NAT. The preparative photolysis of derivative **1d** and NAT afforded two main photoproducts. One of them corresponds to a dimer of decarboxylated NAT. The other is assigned to an adduct of decarboxylated NAT and the quinoxalin-2-one. The structures of the adduct were elucidated by NMR spectroscopic analyses. The ^{1}H NMR showed all of the aromatic protons corresponding to *N*-acetyltryptophan and the quinoxalin-2-one appearing between 6.5 and 8.4 ppm. In addition, two new singlets appeared at low field and are

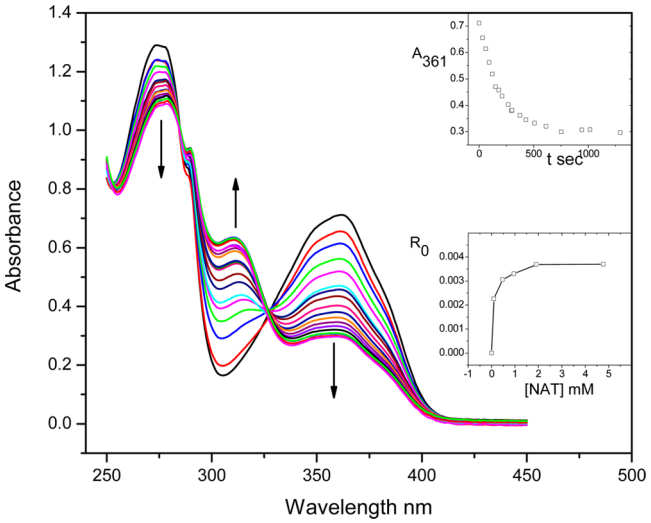

Figure 1. Two isosbestic points at 285 and 326 nm in the photolysis of 0.1 mM CH_3O-substituted derivative **1a** in the presence of 1.9 mM NAT. The arrows show the changes in absorbancies. The upper inset contains the kinetic trace at 361 nm. The lower inset shows the measured initial rates as a function of [NAT].

attributed to the amide NH protons (8.33 and a broad singlet 6.88−6.92 ppm). There were also broad signals at 4.24 and 8.11 ppm that can be attributed to the amine protons (NH). Additional signals at ∼4.54 (dt, 1H), 3.62 (dd, 1H), and 3.02 (dd, 1H) ppm are assigned to the corresponding CH and CH_2 from the tryptophan fragment. Signals at 1.88 (s, 3H) and 1.47 (s, 3H) ppm were assigned to the corresponding protons present in the acetyl (tryptophan fragment) and methyl group in the quinoxalin-2-one ring, respectively. For the ^{13}C NMR, the most important signals appearing at low field (∼170.7 and 170.3 ppm) were attributed to the amide carbonyl carbons. See the experimental section for the complete chemical-shift assignments for the ^{1}H and ^{13}C spectra of the photoproduct and the Supporting Information for the connectivity table. These assignments were obtained by the application of one- and two-dimensional techniques: COSY and long-range two- and three-bond C−H heteronuclear multiple bond connectivity (HMBC).

The most important features of the NMR spectra show the coupling of protons at C3 and C4 showing unambiguously the bound between the decarboxylated NAT and the C at position 3 of the quinoxalin-2-one. The 2D ^{1}H homonuclear COSY spectrum showed the expected two-spin system, at C3 and C4, as two double doublets resonating at 3.02 and 3.62 ppm. The protons at C4, H_c and H_d, are diastereotopic, as expected for a methylene adjacent to a tetrahedral stereocenter (H and C numbering given in Scheme 2 and the Supporting Information). Moreover, in the COSY spectrum it was possible to observe the three-bond coupling between H_d−C−C−H_e, the two-spin system between the double doublet at 3.02, and a double triplet at 4.54 ppm attributed to H_e of the chiral C3. At low field it was possible to assign several couplings, but the most important coupling corresponded to the coupling between H_g (at 7.01 ppm) and H_h (indole N−H_h, 8.11 ppm). By using HMBC spectra, it was possible to identify the quaternary carbons that permitted us to make assignments of the other aromatic signals. The NMR and MS spectra used for the assignment of the photoproducts are included in the Supporting Information.

DOI: 10.1021/acs.jpca.6b01141
J. Phys. Chem. A 2016, 120, 2797−2807

Scheme 2. Adduct Photoproduct and Decarboxylated NAT Dimer

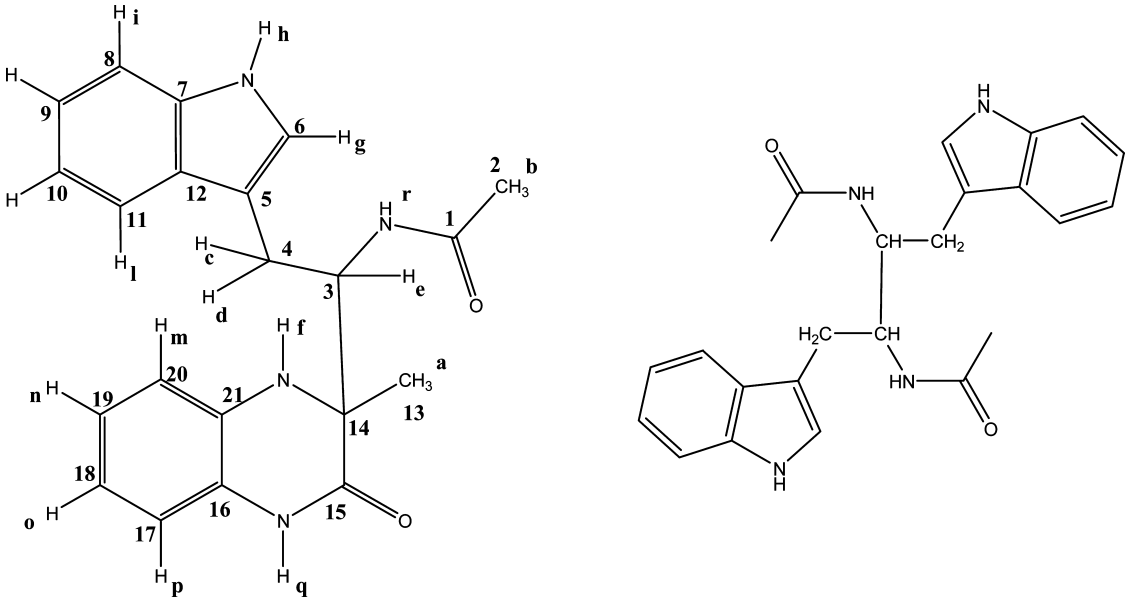

Scheme 3. Possible *N*-Acetyltryptophan Decarboxylation

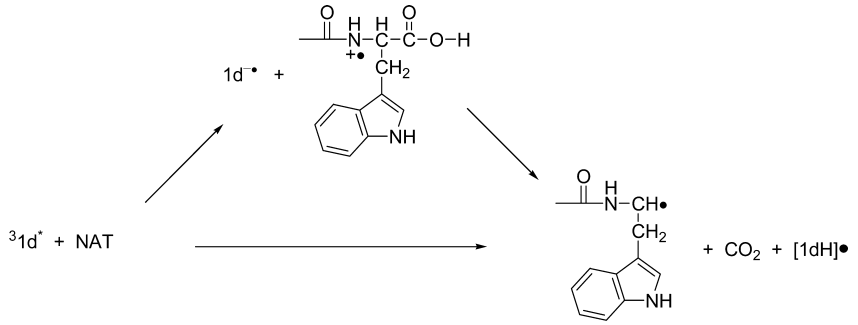

Table 1. Quenching Rate Constants in Acetonitrile

	quinoxalinone substituent						
quencher	CH_3O (**1a**)	CH_3 (**1b**)	F (**1c**)	H (**1d**)	Br (**1e**)	CF_3 (**1f**)	CN (**1g**)
				$k_q/10^9$ M^{-1} s^{-1}			
DABCO	0.07 ± 0.003	0.3 ± 0.03	0.2 ± 0.01	3.9 ± 0.8[a]	0.03 ± 0.001	0.02 ± 0.001	0.9 ± 0.05
NPG	0.5 ± 0.02	1.4 ± 0.04	8.4 ± 0.6[a]	1.5 ± 0.2[a]	7.1 ± 0.04	2.0 ± 0.2[a]	1.4 ± 0.02
NAT	0.9 ± 0.06	1.1 ± 0.03	13.2 ± 0.4[a]	22 ± 0.2[a]	1.9 ± 0.02	1.3 ± 0.04	9.5 ± 0.08

[a]Large error due to the spectral overlap between triplet−triplet absorption and derived radicals.

Photoproducts Mass Analyses. By using HRMS-ESI the molecular ion masses associated with the adduct photoproduct were obtained. In positive mode there was a [M + H] = 363.1808 *m*/*z* (calculated for $C_{21}H_{23}N_4O_2$: 363.1821). Moreover, in the mass spectra, fragments appeared with *m*/*z* 203.1173 and 161.0706, which can be attributed to the decarboxylated *N*-acetyltryptophan fragment [NAT-CO_2 + 2H] (calculated for $C_{12}H_{15}N_2O$: 203.1184) and to the quinoxalin-2-one [**1d** + H] (calculated for $C_9H_9N_2O$: 161.0715).

In addition, the decarboxylated NAT dimer showed in the positive mode a *m*/*z* = 404.2550 compatible with the proposed structure (calculated for $C_{14}H_{28}N_4O_2$ 404.2212).

These results strongly support a decarboxylation of NAT, suggesting a possible electron transfer from the amide N of NAT followed by the decarboxylation of the radical cation $NAT^{\bullet+}$ or alternatively a hydrogen abstraction from the α-C of NAT by the excited quinoxalin-2-one followed by a decarboxylation, as shown in Scheme 3. However, neither of these processes precludes the photoinduced electron transfer from the indoyl moiety of NAT.

Laser Flash Photolysis of Quinoxalin-2-ones in the Presence of NPG. All of the studied 3-methylquinoxalin-2-ones in argon-saturated acetonitrile solution showed transient absorption between 350 and 450 nm with ground depletion at lower wavelengths.

These transient absorptions disappeared completely in aerated solutions and, thus, were assigned to the quinoxalin-2-one triplet excited states, ^{3}**1a−g**. In addition, these absorptions were quenched by DABCO, NPG, and NAT with rate constants close to the diffusion limit, for NPG and NAT, without apparent dependence on the substituents'

DOI: 10.1021/acs.jpca.6b01141
J. Phys. Chem. A 2016, 120, 2797−2807

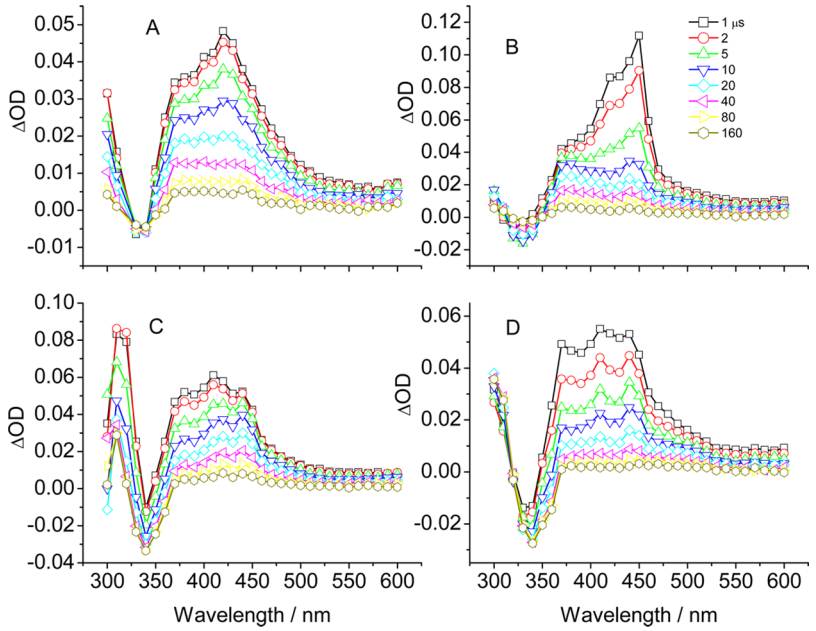

Figure 2. Transient spectra for the 3-methylquinoxalin-2-one CN-derivative **1g** in argon-saturated acetonitrile [**1g**] = 0.1 mM. Panel A: triplet−triplet absorption. Panel B: in the presence of 4.6 mM DABCO. Panel C: in the presence of 2 mM NPG. Panel D: in the presence of 2 mM NAT. All the transient spectra were obtained at the same elapsed times shown in panel B.

nature, Table 1. In general, the quenching constant are in line with the reduction potential of the electron donor: 0.84, 0.89, and 1.23 V v/s NHE for DABCO,[49] NPG,[27,38] and NAT,[40] respectively. Therefore, the quenching process might be mainly attributed to SET, however, without disregarding a possible hydrogen transfer from the amino acid to the quinoxalin-2-one excited triplets that might explain the higher k_q constants of amino acids with respect to DABCO.

Some of these quenching constants have a large associated error due to the close spectral overlap between the triplet absorption and those of the transient generated in the presence of the quenchers. An example of the observed transient absorptions is shown for the CN-substituted quinoxalin-2-one, **1g**, in Figure 2.

Panel A of the figure shows the ^{3}**1g** triplet−triplet absorption with a maximum at 420 nm and a shoulder at 370 nm and negative absorptions due to ground-state depletion near 330 nm. These absorptions decayed monotonically with a lifetime $\tau = 20 \pm 2$ μs.

With the addition of [DABCO] = 4.6 mM, assuring nearly the total quenching of the excited triplet, Figure 2B, the transient spectra changed notably showing a maximum at 450 nm, two shoulders; one at 420 nm and the second at 370−380 nm that evolved into a second maximum at longer elapsed times (>10 μs), suggesting the formation of a second species. It is noteworthy that the maximal absorption was nearly 2.3 times larger than those for the triplet. In the presence of 2 mM NPG, a broad band with two maxima at 410 and 315 nm and shoulders at 380 and 440 nm was observed, Figure 2C. A close inspection of these absorptions reveal that they decayed distinctly, as can be seen from the ratios $\Delta OD_{1\mu s}/\Delta OD_{40\mu s}$ that take values of 2.6, 3.2, 4.3, and 2.5 at 440, 410, 380, and 310 nm, respectively. These ratios show clearly the simultaneous decay of at least three transient species. Figure 2D shows the transient spectra of **1g** in the presence of 2 mM NAT, again, a broad absorption band was observed with maximum at 410 nm with shoulders at 440 and 370 nm, and with a tail between 450−530 nm evolving at different rates. Among these spectral features, there was a nondescript absorption with maximum below 300 nm. The close resemblance between the transient spectra maxima obtained with NPG and NAT suggest that, in both cases, similar species should be present, at least for the quinoxalin-2one derivate. The transient spectra for all of the other substituted quinoxalin-2-ones in the presence of DABCO, NPG, and NAT showed similar behavior, suggesting again that at least three species were formed and decayed simultaneously in the presence of NPG and NAT.

It is well know that DABCO is a good electron donor whose radical cation DABCO$^{\bullet+}$ decays by back electron transfer without further reaction. The expected DABCO$^{\bullet+}$ absorption at 465 nm[50,51] (ε = 2100 $M^{-1}cm^{-1}$)[52] is not discernible in our experimental spectra as well as on other reported photoreductions by DABCO.[16,53−55] In the photoreduction by DABCO of 4,4′-bypyridine[56,57] the absorption of DABCO$^{\bullet+}$ does not contribute significantly to the transient spectra, even at very short times after laser pulse. Therefore, the spectra of quinoxalin-2-ones in the presence of DABCO should be assigned to the respective **1a−g** radical anion, eq 1. The radical ion pair should decay monoexponentially by back electron transfer, eq 2.

$$^3\mathbf{1a{-}g} + \text{DABCO} \rightarrow [\mathbf{1a{-}g}]^{\bullet-} + \text{DABCO}^{\bullet+} \quad (1)$$

$$[\mathbf{1a{-}g}]^{\bullet-} + \text{DABCO}^{\bullet+} \rightarrow \mathbf{1a{-}g} + \text{DABCO} \quad (2)$$

As we stated above, a strong absorption with a maximum at 450 nm was evident when **1g** was quenched by DABCO, and at elapsed times $t > 10$ μs, a new absorption band centered at 370 nm developed. This last band was attributed to the neutral quinoxalin-2-one radical [**1a−g**]H$^{\bullet}$ generated by the protonation of the radical anion by H$^+$ coming from adventitious sources and/or added water to the solution, as we reported early,[13] eq 3. This assignment is compatible with the spectral

DOI: 10.1021/acs.jpca.6b01141
J. Phys. Chem. A 2016, 120, 2797−2807

Scheme 4. Quinoxalin-2-one Derived Radicals and Simplified Reaction Scheme

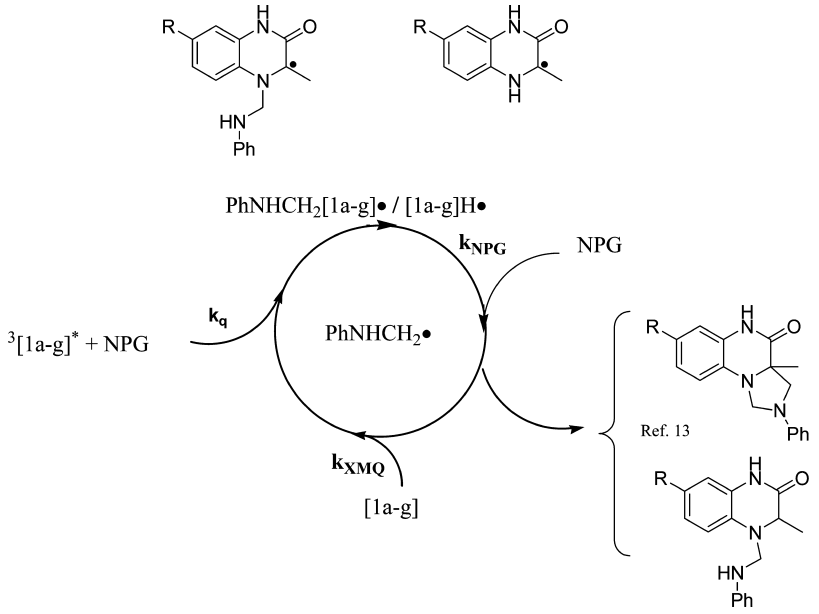

features of species $[\mathbf{1d}]H^{\bullet}/[\mathbf{1d}]^{\bullet-}$ in water recently reported by Skotnicki et al.[15]

$$[\mathbf{1a-g}]^{\bullet-} + H^{+} \rightarrow [\mathbf{1a-g}]H^{\bullet} \quad (3)$$

In the presence of NPG, whose radical cation decarboxylates easily, the sequence of reactions of eqs 4−6 should be considered. Therefore, the species contributing to the transient absorption in the solutions containing quinoxalin-2-one and NPG should be $NPG^{\bullet+}$ and $[\mathbf{1a-g}]^{\bullet-}$ at short times after the pulse, followed at longer times by the absorptions of the protonated radical anion: $[\mathbf{1a-g}]H^{\bullet}$ and $PhNHCH_2^{\bullet}$ and other intermediate radicals species, shown in Scheme 4, leading to the reported imidazoquinoxalin-2-ones.[13]

$$^{3}\mathbf{1a-g} + NPG \rightarrow [\mathbf{1a-g}]^{\bullet-} + NPG^{\bullet+} \quad (4)$$

$$NPG^{\bullet+} \rightarrow PhNHCH_2^{\bullet} + CO_2 + H^{+} \quad (5)$$

$$[\mathbf{1a-g}]^{\bullet-} + H^{+} \rightarrow [\mathbf{1a-g}]H^{\bullet} \quad (6)$$

By subtracting the spectral contributions of the radical anions $[\mathbf{1a-g}]^{\bullet-}$, obtained in the presence of DABCO, from the spectra in the presence of NPG, we isolated the contributions of the other species contributing to the transient absorption. This is a common method to make evident the presence of different species that we used successfully in previous works.[45,54,58] In Figure 3 are shown the transient spectra of the CF_3 derivative **1f** in the presence of NPG and DABCO and the difference between them. In the presence of NPG, Figure 3A, two maxima at 315 and 430 nm together with two shoulders between 350 and 430 nm appear. With DABCO, Figure 3B, at short times, a pronounced maximum at 430 nm and shoulders at 420 and 370 appear immediately after the laser pulse and can be attributed to the radical anion $[\mathbf{1f}]^{\bullet-}$. This absorption evolved at longer elapsed times into a well-defined band around 380 nm. This last spectrum was assigned previously to the quinoxalin-2-one protonated radical cation $[\mathbf{1f}]H^{\bullet}$ due to their behavior with added H_2O.[13] As the radical anion absorption was more intense than those obtained with NPG, likely due to the fast competitive decay processes that

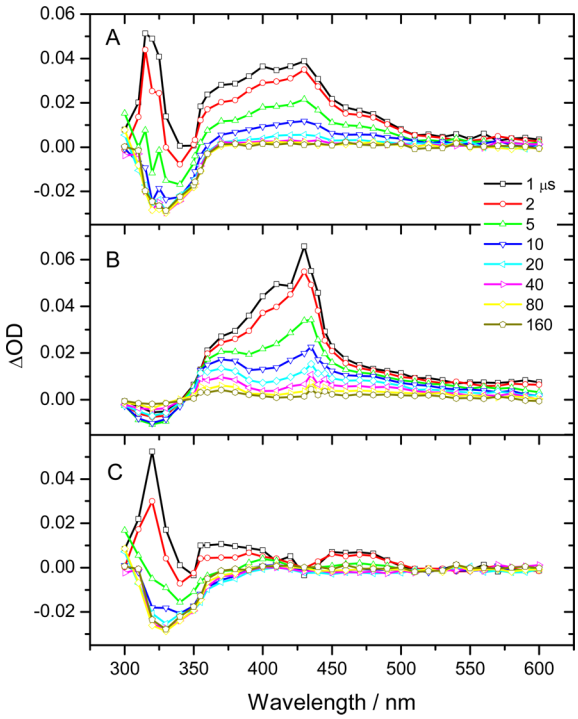

Figure 3. Transient spectra of 0.1 mM CF_3-derivative **1f** in the presence of (A) 3.9 mM NPG, (B) 4.3 mM DABCO, and (C) transient spectra obtained from the subtraction of normalized spectra in (B) from spectra in (A).

deactivate and consume the radical anion $[\mathbf{1f}]^{\bullet-}$, eqs 4−6, or to a H transfer quenching, similar to those proposed for NAT that cannot be ruled out for NPG, it is necessary to normalize it before subtracting to obtain the difference spectra, Figure 3C. These difference spectra clearly show absorption corresponding to $NPG^{\bullet+}$ between 440 and 500 nm[38] and a broad absorption between 360 and 420 nm that should be ascribed to the quinoxalin-2-one neutral radical $[\mathbf{1f}]H^{\bullet}$. The strong absorption with a maximum at 315 nm (Figure 3A,C) has to be attributed to $PhNHCH_2^{\bullet}$.[37] It is noteworthy that transient spectra in the

DOI: 10.1021/acs.jpca.6b01141
J. Phys. Chem. A 2016, 120, 2797−2807

presence of DABCO showed an important contribution of [**1f**]H$^{\bullet}$ absorption after 5 μs, Figure 3B. Thus, in the difference spectra (Figure 3C) the [**1f**]H$^{\bullet}$ absorption between 350 and 380 nm should be deemphasized.

For all of the quinoxalin-2-ones in the presence of NPG, similar difference spectra were obtained, with a more or less pronounced absorption of NPG$^{\bullet+}$ between 450 and 500 nm, the distinctive absorption maximum attributed to PhNHCH$_2^{\bullet}$ at 315 nm and a strong negative absorption between 320 and 360 nm at longer elapsed times. This latter spectral feature is due to the consumption of the quinoxalin-2-ones in their ground state. The kinetic traces of these absorptions at 315 and 320−360 nm were used to study the reported radical chain reaction between **1a−g** and NPG.[13]

Kinetic of Photoreaction between Quinoxalin-2-ones and NPG. The kinetic traces of the different species observed in the photoreduction of quinoxalin-2-ones, **1a−g**, by NPG provide valuable information concerning the kinetic processes that involve the transient species. One of the more prominent features of all of the transient spectra obtained in the presence of NPG was the presence of the strong absorption band attributed to PhNHCH$_2^{\bullet}$ at 315 nm. This absorption increased its intensity and growth rate constants with the increase of [NPG], as is shown in Figure 4 for the CF$_3$ derivative **1f**.

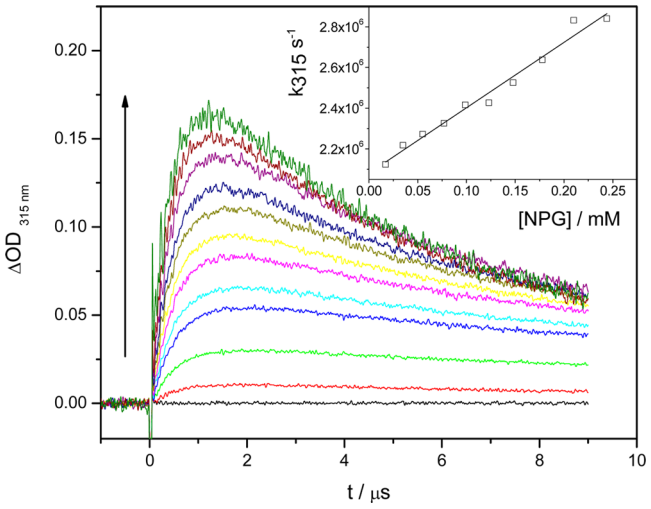

Figure 4. Absorption traces of PhNHCH$_2^{\bullet}$ at 315 nm in function of NPG concentration for 0.1 mM 7-CF$_3$ derivative **1f**. The arrow shows increasing [NPG]. Inset: dependence on [NPG] of pseudo-first-order growth rate constants at 315 nm. The slope of this plot yields the second-order rate constant k(PhNHCH$_2^{\bullet}$) = (3.22 ± 0.16) × 10^9 M^{-1} s^{-1}.

From the 315 nm absorbance traces in Figure 4, it can be seen that both their maximal intensities and their rates of growth increase in [NPG]. The growth rate constants were evaluated by fitting the monoexponential growths up to their respective absorption maxima. Plotting these pseudo-first-order rate constants at 315 nm, k_{315}, vs the NPG concentration as shown in the inset of Figure 4 resulted in a linear behavior. For all of the derivatives **1a−f** the same linear behavior was observed. From the slope of these linear plots, the second-order rate constants for the generation of PhNHCH$_2^{\bullet}$, k(PhNHCH$_2^{\bullet}$), were evaluated. All of them had values close to the diffusion limit without any apparent relationship to the substituents. See Table 2.

The other common feature observed in the transient spectra of all of the investigated 3-methylquinoxalin-2-one derivatives in the presence of NPG is the ground depletion bleaching observed between 320 and 360 nm, depending on the substituent. Both the bleaching amplitude and the initial monoexponential quinoxalin-2-one consumption rate constant depended on the NPG and the quinoxalin-2-one concentrations as shown in Figure 5 for derivative **1d**. These data allowed us to estimate the kinetic contributions of NPG and quinoxalin-2-one on the consumption of quinoxalin-2-one.

For the effect of [NPG] on the bleaching of the **1d** derivative, the slope and intercept Figure 5A are k_{NPG} = (1.59 ± 0.12) × 10^7 M^{-1} s^{-1} and $1/\tau_1$ = (1.44 ± 0.1) × 10^4 s^{-1}, respectively. For the effect of the [**1d**] on the bleaching, the slope was k_{XMQ} = (1.47 ± 0.08) × 10^8 M^{-1} s^{-1}, and the intercept was $1/\tau_2$ = (8.07 ± 0.2) × 10^4 s^{-1} (Table 2). These slope values show that the quinoxalin-2-one **1d** accelerated its own consumption nearly 10 times faster than did the NPG. The intercepts can be interpreted as the first-order decay rate constants of the intermediates that were responsible for the quinoxalin-2-one consumption. The lifetimes of these intermediates are τ_1 = 70 and τ_2 = 12 μs for the consumption reactions depending on NPG and **1d**, respectively. These lifetimes could be related to the intermediates of Scheme 4 and to PhNHCH$_2^{\bullet}$. Both of the quinoxalin-2-one derived radicals are likely able to oxidize NPG to NPG$^{\bullet+}$ or abstract hydrogen from the NPG to PhNHCH·COOH in both cases leading to PhNHCH$_2^{\bullet}$ by decarboxylation. This latter species, the α-aminoalkyl radical is known as a strong one-electron reductant and therefore able to reduce the quinoxalin-2-one as we proposed earlier.[13]

In the present experimental conditions we were not able to distinguish the intermediates of Scheme 4. Nevertheless, probably these are the long-lived intermediates that react ten times slower that the short-lived intermediate, the more reactive PhNHCH$_2^{\bullet}$ (Table 2), This reactivity might be related

Table 2. Observed Dependence on NPG Concentration of Second-Order Rate Constant, k(PhNHCH$_2^{\bullet}$), for the Growth of the PhNHCH$_2^{\bullet}$ Radical Absorption at 315 nm[a]

	substituent						
derivative X	CH$_3$O (**1a**)	CH$_3$ (**1b**)	F (**1c**)	H (**1d**)	Br (**1e**)	CF$_3$ (**1f**)	CN (**1g**)
k(PhNHCH$_2^{\bullet}$)/10^9 M^{-1}s^{-1}	0.99 ± 0.03	1.06 ± 0.03	1.21 ± 0.07	1.16 ± 0.03	0.85 ± 0.04	3.22 ± 0.16	1.59 ± 0.08
k_{NPG} /10^{7}M^{-1} s^{-1}	2.58 ± 0.13			1.59 ± 0.12		3.57 ± 0.27	
τ_1/μs	27.8			69.4		6.8	
k_{XMQ}/10^{8}M^{-1} s^{-1}	1.48 ± 0.06			1.47 ± 0.08		2.01 ± 0.27	
τ_2/μs	16.4			12.4		9.3	

[a]Bimolecular kinetic rate constant depending on [NPG], k_{NPG}; and on quinoxalin-2-one derivative concentration [XMQ], k_{XMQ}; and the lifetime of intermediates PhNHCH$_2$[**1a−g**]$^{\bullet}$/[**1a−g**]H$^{\bullet}$, Scheme 4, τ_1, and PhNHCH$_2^{\bullet}$, τ_2.

DOI: 10.1021/acs.jpca.6b01141
J. Phys. Chem. A 2016, 120, 2797−2807

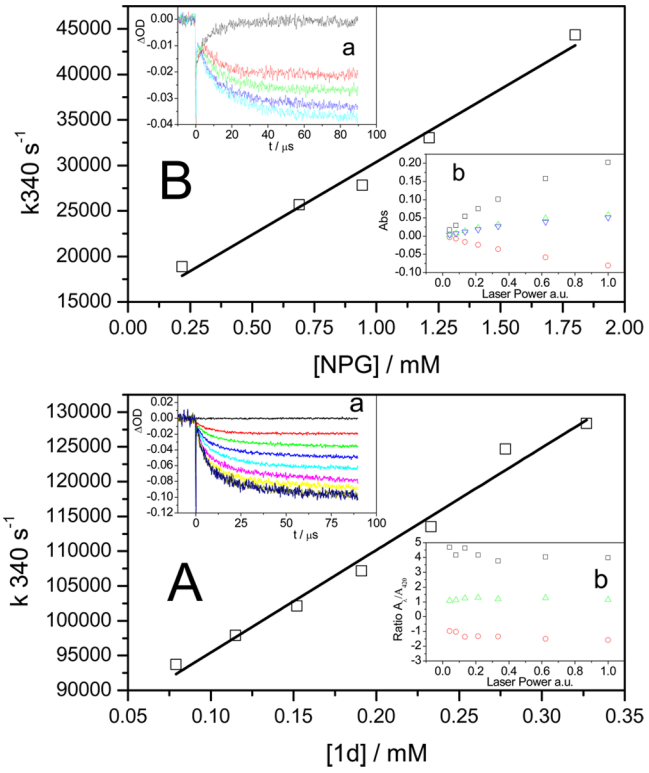

Figure 5. (A) Effect of NPG concentration on pseudo-first-order rate constant for the bleaching of 0.08 mM 3-methylquinoxalin-2-one **1d** measured at 340 nm. (a) shows the kinetic traces at increasing [NPG]. (b) shows the maximal intensity observed at wavelengths 315 (□), 340 (○), 360, (△), and 420 (▽) nm at increasing laser powers (see text for explanation). (B) Effect of addition of derivative **1d** to solutions containing 2.4 mM [NPG] in the bleaching pseudo-first-order rate constants. (a) contains the kinetic traces at 340 nm from which the rate constants were extracted. (b) shows the maximal absorptions ratios $A_\lambda/A_{420\ nm}$ for wavelengths 315 (□), 340 (○), and 360 (△) nm (see explanation in the text).

to the steric hindrance of radicals $PhNHCH_2Q^\bullet$ and $QH^\bullet$ compared with the α-amino-alkyl radical $PhNHCH_2^\bullet$, which is able to attack the ground state of quinoxalin-2-one at C3 or N4. For the other quinonoxalin-2-one derivatives, similar effects were observed and evaluated for the derivatives **1a** and **1f**. These data are included in Table 2.

To disregard possible two photon processes, we studied the effect of laser power on the maximal transient absorptions corresponding to $PhNHCH_2^\bullet$, the bleaching of **1d**, the protonated radical anion $[\mathbf{1d}]H^\bullet$, and the radical anion appearing at 315, 340, 360, and 420 nm, respectively. The intensity of these absorptions, as expected, increased with the laser power as shown in Figure 5A (inset b). The same absorptions when normalized by the absorption of radical anion did not change with the laser power Figure 5B (inset b). The nearly constant behavior observed ruled out multiphotonic absorption processes affecting the generation of the transient species.

Laser Flash Photolysis of Quinoxalin-2-ones in the Presence of NAT. Even though the product formation of the adduct was between the decarboxylated NAT and the quinoxalin-2-one through a SET from the amide NH or an H abstraction from the α-C of NAT, electron transfer can also occur from the indoyl N, as suggested in the study of the transient spectra in the presence of NAT. By assuming that the first process for the excited-state quinoxalin-2-ones and NAT is a photoinduced SET from the NAT to **1a**−**g**, eq 7, the contribution of the quinoxalin-2-one radical anion $[\mathbf{1a-g}]^{\bullet-}$, obtained in the presence of DABCO can be subtracted from the transient spectra in the presence of NAT. By applying this procedure, it should be possible to identify the transient radical species derived from NAT in the resulting difference spectra.

As stated before, from the SET, it can be expected that there would be an appearance of $NAT^{\bullet+}$ with an absorption maximum at 560 nm for the indoyl radical cation.[40,45,46,59] The pK_a of this indoyl radical cation, $NAT^{\bullet+}$ should be similar to those reported for tryptophan (4.3),[40] *N*-acetyltryptophanamide (4.3).[46] Thus, it can be expected that there would be a lost of H^+ from the NAT indole nitrogen,[40] eq 8. This deprotonated radical, $[NAT\text{-}H]^\bullet$, has a reported absorption centered at 510 nm,[45,60] similar to those presented by the tryptophanyl radical $Trp\text{-}H^\bullet$.[39,40,61]

In the presence of $[\mathbf{1a-g}]^{\bullet-}$ proton transfer from $NAT^{\bullet+}$ should take place with the formation of the respective $[\mathbf{1a-g}]H^\bullet$ and $[NAT\text{-}H]^\bullet$, eq 9.

$$^3\mathbf{1a-g} + NAT \rightarrow [\mathbf{1a-g}]^{\bullet-} + NAT^{\bullet+} \quad (7)$$

$$NAT^{\bullet+} \leftrightarrow [NAT\text{-}H]^\bullet + H^+ \quad (8)$$

$$NAT^{\bullet+} + [\mathbf{1a-g}]^{\bullet-} \rightarrow [NAT\text{-}H]^\bullet + [\mathbf{1a-g}]H^\bullet \quad (9)$$

Furthermore, the $NAT^{\bullet+}$ with the radical located in the amide N should give rise to the decarboxylated NAT radical $[NAT\text{-}CO_2]^\bullet$, as shown in eq 10 eventually generating the observed product.

$$NAT^{\bullet+} \rightarrow [NAT\text{-}CO_2]^\bullet + CO_2 + H^+ \quad (10)$$

In Figure 6 are shown the transient spectra for the 7-methoxy-3-methylquinoxalin-2(1*H*)-one derivative **1a** in the presence of 2.2 mm NAT and 4.6 mM DABCO and the difference spectra, Figure 6A−C, respectively. In the presence of NAT, Figure 6A, a maximum at 450 nm appears 2 μs after the laser pulse. Together with this maximum, a relatively strong absorption below 350 nm and two not well-defined shoulders at 400 and 500 nm appear, with a tail extending to 570 nm. In the presence of DABCO, Figure 6B, a broad and strong absorption with a maximum at 460 nm and a shoulder at 430 nm appear shortly after the laser pulse. These absorptions evolve into two bands with maxima at 420 and 520 nm at elapsed times larger than 40 μs. At these long elapsed times, the absorption at 420 nm can be attributed to the quinoxalin-2-one protonated anion radical $[\mathbf{1a}]H^\bullet$, generated by proton transfer from $NAT^{\bullet+}$ to the respective quinoxalin-2-one radical anion, eq 9.

It is clear from these spectra, in the presence of NAT or DABCO, that the strong absorption overlap between them does not allow an easy transient spectral assignment. However, the difference spectra, Figure 6C, show clearly the contribution of NAT derived transients. The broad band between 470 and 540 nm can be attributed to the deprotonated NAT indoyl radical cation, $[NAT\text{-}H]^\bullet$, and the absorption between 390 and 420 nm with a maximum at 410 nm can be assigned to the quinoxalin-2-one neutral hydrogenated radical $[\mathbf{1a}]H^\bullet$, while the nondescript absorption growing in below 300 nm might probably be due to the NAT decarboxylated radical $[NAT\text{-}CO_2]^\bullet$.

The preceding spectral assignments have been made by subtracting the contribution of the quinoxalin-2-one radical anion $[\mathbf{1a}]^{\bullet-}$ from the total absorption in the presence of NAT.

DOI: 10.1021/acs.jpca.6b01141
J. Phys. Chem. A 2016, 120, 2797−2807

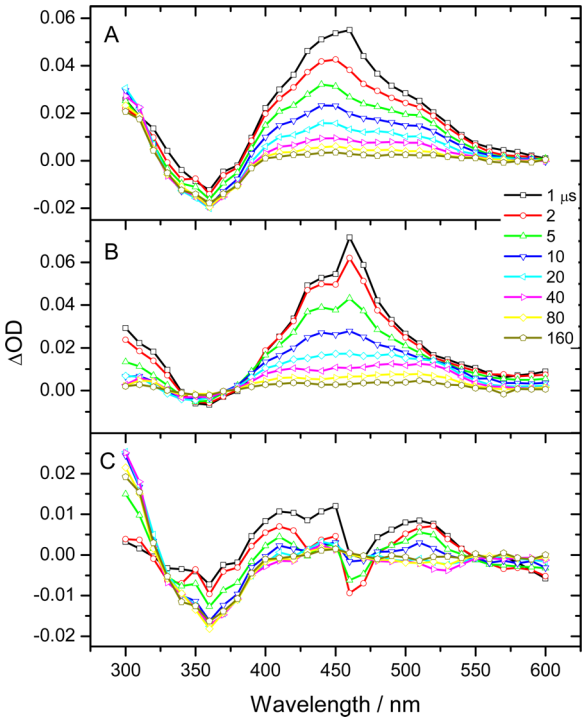

Figure 6. Transient spectra of 0.1 mM CH_3O derivative **1a** in the presence of (A) 2.2 mM NAT and (B) 4.6 mM DABCO and (C) transient spectra obtained from the subtraction of normalized spectra in (C) from spectra in (A).

Therefore, these results are an indirect probe that the reaction between NAT and the excited triplet quinoxalin-2-ones proceeded at least partially through a SET from the indoyl N to the triplet excited state of the quinoxalin-2-one. This process should be followed by the proton-transfer reaction 9 leading to $[NAT\text{-}H]^{\bullet}$ and $[\mathbf{1a-g}]H^{\bullet}$.

The spectral behavior for all of the 7-substituted quinoxalin-2-ones in the presence of NAT and DABCO are similar. For example, the differential spectra obtained for the 7-F-substituted quinoxalin-2-one **1c**, Figure 7, shows clearly that $[NAT\text{-}H]^{\bullet}$ absorbing at 510 nm and $[\mathbf{1c}]H^{\bullet}$ at 410 nm are formed synchronously with the decay of $[\mathbf{1c}]^{\bullet-}$ at 440 nm.

It is interesting to note that the absorption at 510 nm, attributed to the indoyl deprotonated radical $[NAT\text{-}H]^{\bullet}$, Figure 7 inset, which grew initially with the laser pulse, has a secondary growth, with a rate constant of $9.1 \times 10^5\ s^{-1}$, which matches within the experimental error with the decay of $[\mathbf{1c}]^{\bullet-}$ at 440 nm. These facts indicate that the first steps of the photoreduction of quinoxalin-2-ones by NAT can be adequately represented by eqs 7 and 9. However, the decarboxylation (Scheme 3 and eq 10), leading to the radical adduct photoproduct, should also be considered. Likely, this process has a low efficiency and is fast enough not to allow the direct observation of the $NAT^{\bullet+}$ located in the amide N or the α-C NAT radical.

As we stated earlier, the measured quinoxalin-2-one photoconsumption quantum yields by NAT, all lower than unity, eliminate the possibility of a radical chain reaction and do not reveal relationship with the substituent electronic properties. Moreover, these quinoxalin-2-one photoconsumption quantum yields are not necessarily related to formation of stable photoproducts that likely occurs via the attack of $[NAT\text{-}CO_2]^{\bullet}$ on the ground-state quinoxalin-2-one.

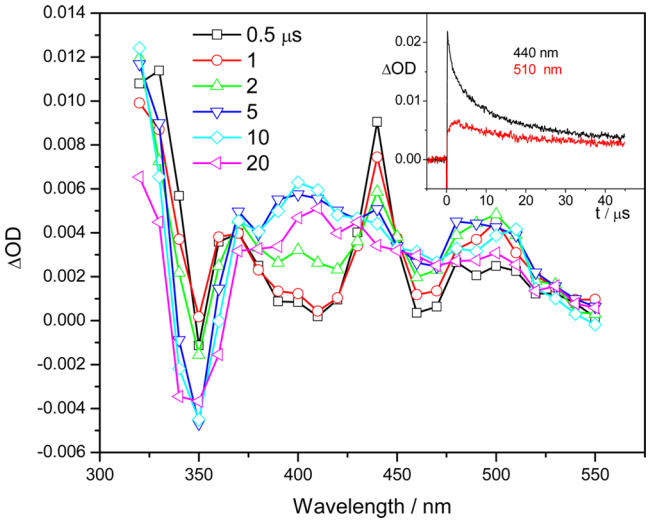

Figure 7. Differential transient spectra for 7-F quinoxalin-2-one derivative **1c** obtained from the subtraction of radical anion spectra $[\mathbf{1c}]^{\bullet-}$ in the presence of 4.3 mM DABCO from the transient spectra obtained in the presence of 2.2 mM NAT. The inset shows the decay profiles of **1c** in the presence of 2.2 mM NAT at 410 nm (black) and the growth and decay of $[NAT\text{-}H]^{\bullet}$ at 510 nm (red).

CONCLUSIONS

Transient intermediates for the photoreduction of 3-methylquinoxalin-2-one derivatives by NPG and NAT were identified. For both reductants a sequence of reactions was postulated that comprise first a photoinduced single electron transfer followed by a proton transfer from the radical cation of the electron donor to the radical anion of the 3-methylquinoxalin-2-one. This initial sequence gave rise to the observed products, i.e., the imidazoquinoxalin-2-ones for the reaction with NPG and the adduct between the quinoxalin-2-one and decarboxylated *N*-acetyltryptophan for the NAT. As far as we know, this is the first report of NAT decarboxylation unambiguously supported by stable products characterization following photolysis. There are many proteins in which a C-terminal tryptophan plays an essential role in the function of the protein and its alteration might have severe consequences at the cellular and the whole organism levels. An example is the C-terminus tryptophan of the chaperon protein TBCE, where the replacement of tryptophan for other amino acid is associated with neurodegenerative diseases such as amyotrophic sclerosis.[62] Also the alteration of C-terminal tryptophan have been associated with leukemia and myeloid leukemia,[63,64] biological electron transport,[65,66] and virus activity.[67] Moreover, a possible H abstraction at the α-C of non-C-terminal tryptophan leaving a C centered radical might cause severe damages in proteins.

We quantified the effect of the concentration of NPG and the quinoxalin-2-one on the rate of their photoconsumption and estimated the possible intermediates' lifetimes accounting for these processes supporting our previous assumption[13] that the proposed radical chain reaction was modulated by the reaction of $PhNHCH_2^{\bullet}$ with the ground-state 3-methylquinoxalin-2-ones. In the photoreduction by NAT, the evident formation of the indoyl deprotonated radical $[NAT\text{-}H]^{\bullet}$ via a delayed process confirmed that the photoinduced single electron transfer from the NAT to the substituted 3-methylquinoxalin-2-one excited triplet state is one of the paths involved in the photoreduction.

DOI: 10.1021/acs.jpca.6b01141
J. Phys. Chem. A 2016, 120, 2797−2807

■ ASSOCIATED CONTENT

Supporting Information

The Supporting Information is available free of charge on the ACS Publications website at DOI: 10.1021/acs.jpca.6b01141.

Adduct structure and NMR connectivity table and NMR and mass spectra used for the characterization of the adduct of 3-methylquinoxalin-2-one and decarboxylated NAT product (PDF)

■ AUTHOR INFORMATION

Corresponding Author

*Julio R. De la Fuente. Phone: (56-2) 2978-2880. Fax: (56-2)-2978-2868. E-mail: jrfuente@ciq.uchile.cl.

Notes

The authors declare no competing financial interest.

■ ACKNOWLEDGMENTS

We are thankful for the financial support of FONDECYT grant No. 1150576, for Universidad de Chile VID grant No. ENL013/14, to Prof. G. Hug from NDRL for the critical reading of our manuscript, and to M. de los Angeles Juricic U. for their valuable biochemical hints.

■ REFERENCES

(1) Kamila, S.; Biehl, E. R. Synthetic Studies of Bioactive Quinoxalinones: A Facile Approach to Potent Euglycemic and Hypolipidemic Agents. *Heterocycles* **2006**, *68*, 1931.

(2) Olayiwola, G.; Obafemi, C. A.; Taiwo, F. O. Synthesis and Neuropharmacological Activity of Some Quinoxalinone Derivatives. *Afr. J. Biotechnol.* **2007**, *6*, 777.

(3) Gris, J.; Glisoni, R.; Fabian, L.; Fernandez, B.; Moglioni, A. G. Synthesis of Potential Chemotherapic Quinoxalinone Derivatives by Biocatalysis or Microwave-Assisted Hinsberg Reaction. *Tetrahedron Lett.* **2008**, *49*, 1053.

(4) Carta, A.; Piras, S.; Loriga, G.; Paglietti, G. Chemistry, Biological Properties and Sar Analysis of Quinoxalinones. *Mini-Rev. Med. Chem.* **2006**, *6*, 1179.

(5) Matuszczak, B.; Mereiter, K. Syntheses in the Series of Pyrazolyl-Substituted Quinoxalines. *Heterocycles* **1997**, *45*, 2449.

(6) Matuszczak, B.; Pekala, E.; Muller, C. E. 1-Substituted 4-[Chloropyrazoly][1,2,4]Triazolo[4,3-a]Quinoxalines: Synthesis and Structure-Activity Relationships of a New Class of Benzodiazepine and Adenosine Receptor Ligands. *Arch. Pharm.* **1998**, *331*, 163.

(7) Dudash, J.; Zhang, Y. Z.; Moore, J. B.; Look, R.; Liang, Y.; Beavers, M. P.; Conway, B. R.; Rybczynski, P. J.; Demarest, K. T. Synthesis and Evaluation of 3-Anilino-Quinoxalinones as Glycogen Phosphorylase Inhibitors. *Bioorg. Med. Chem. Lett.* **2005**, *15*, 4790.

(8) Ivanova, A. E.; Khudina, O. G.; Burgart, Y. V.; Saloutin, V. I. Synthesis of Regioisomeric N- and O-Alkylated 3-Polyfluoroalkyl-1,2-Dihydroquinoxalin-2-Ones. *Russ. Chem. Bull.* **2011**, *60*, 937.

(9) Sun, L.-R.; Zhong, J. L.; Cui, S.-X.; Li, X.; Ward, S. G.; Shi, Y.-Q.; Zhang, X.-F.; Cheng, Y.-N.; Gao, J.-J.; Qu, X.-J. Modulation of P-Glycoprotein Activity by the Substituted Quinoxalinone Compound Qa3 in Adriamycin-Resistant K562/A02 Cells. *Pharmacol. Rep.* **2010**, *62*, 333.

(10) Ingale, S. J.; Gupta, S.; Upmanyu, N.; Pande, M. Synthesis and Biological Evaluation of Some 4-Substituted Quinoxalinones. *Asian J. Chem.* **2007**, *19*, 3797.

(11) Xu, B.; Sun, Y.; Guo, Y.; Cao, Y.; Yu, T. Synthesis and Biological Evaluation of N4-(Hetero)Arylsulfonylquinoxalinones as Hiv-1 Reverse Transcriptase Inhibitors. *Bioorg. Med. Chem.* **2009**, *17*, 2767.

(12) Zimpl, M.; Skopalova, J.; Jirovsky, D.; Bartak, P.; Navratil, T.; Sedonikova, J.; Kotoucek, M. Electrochemical Behavior of Quinoxalin-2-One Derivatives at Mercury Electrodes and Its Analytical Use. *Sci. World J.* **2012**, *2012*, 409378.

(13) De la Fuente, J. R.; Cañete, Á.; Jullian, C.; Saitz, C.; Aliaga, C. Unexpected Imidazoquinoxalinone Annulation Products in the Photoinitiated Reaction of Substituted-3-Methyl-Quinoxalin-2-Ones with N-Phenylglycine. *Photochem. Photobiol.* **2013**, *89*, 1335.

(14) Skotnicki, K.; De la Fuente, J.; Cañete, A.; Bobrowski, K. Spectral and Kinetic Properties of Radicals Derived from Oxidation of Quinoxalin-2-One and Its Methyl Derivative. *Molecules* **2014**, *19*, 19152.

(15) Skotnicki, K.; De la Fuente, J. R.; Cañete, A.; Bobrowski, K. Radiation-Induced Reduction of Quinoxalin-2-One Derivatives in Aqueous Solutions. *Radiat. Phys. Chem.* **2016**, *124*, 91.

(16) De la Fuente, J. R.; Cañete, A.; Saitz, C.; Jullian, C. Photoreduction of 3-Phenylquinoxalin-2-Ones by Amines: Transient-Absorption and Semiempirical Quantum-Chemical Studies. *J. Phys. Chem. A* **2002**, *106*, 7113.

(17) De la Fuente, J. R.; Cañete, A.; Zanocco, A. L.; Saitz, C.; Jullian, C. Formal Hydride Transfer Mechanism for Photoreduction of 3-Phenylquinoxalin-2-Ones by Amines. Association of 3-Phenylquinoxalin-2-One with Aliphatic Amines. *J. Org. Chem.* **2000**, *65*, 7949.

(18) Kucybala, Z.; Paczkowski, J. 3-Benzoyl-7-Diethylamino-5-Methyl-1-Phenyl-1h-Quinoxalin-2-One: An Effective Dyeing Photoinitiator for Free Radical Polymerization. *J. Photochem. Photobiol., A* **1999**, *128*, 135.

(19) Nishio, T. Photocycloaddition of Quinoxaline-2(1h)-Thiones to Alkenes. *Helv. Chim. Acta* **1992**, *75*, 487.

(20) Nishio, T.; Kondo, M.; Omote, Y. Photochemical-Reactions of Tetrahydroquinoxalin-2(1h)-Ones and Related Compound. *Helv. Chim. Acta* **1991**, *74*, 225.

(21) Nishio, T. Photochemical-Reactions of Quinoxalin-2-Ones and Related-Compounds. *J. Chem. Soc., Perkin Trans. 1* **1990**, 565.

(22) Nishio, T.; Omote, Y. Photocycloaddition of Quinoxalin-2-Ones and Benzoxazin-2-Ones to Aryl Alkenes. *J. Chem. Soc., Perkin Trans. 1* **1987**, 2611.

(23) Nishio, T.; Omote, Y. Photochemical Reductive Dimerization of Quinoxalin-2-Ones and 1,4-Benzoxazin-2-One. *J. Chem. Soc., Chem. Commun.* **1984**, 1293.

(24) Nishio, T. The (2 + 2) Photocycloaddition of the Carbon-Nitrogen Double Bond of Quinoxalin-2(1h)-Ones to Electron-Deficient Olefins. *J. Org. Chem.* **1984**, *49*, 827.

(25) Brimage, D. R. G.; Davidson, R. S.; Steiner, P. R. Use of Heterocyclic Compounds as Photosensitisers for the Decarboxylation of Carboxylic Acids. *J. Chem. Soc., Perkin Trans. 1* **1973**, 526.

(26) Brimage, D. R. G.; Davidson, R. S. Photoreactions of Polycyclic Aromatic Hydrocarbons with N-Arylglycines. *J. Chem. Soc., Perkin Trans. 1* **1973**, 496.

(27) Ikeda, S.; Murata, S. Photolysis of N-Phenylglycines Sensitized by Polycyclic Aromatic Hydrocarbons - Effects of Sensitizers and Substituent Groups and Application to Photopolymerization. *J. Photochem. Photobiol., A* **2002**, *149*, 121.

(28) Ikeda, S.; Murata, S.; Ishii, K.; Hamaguchi, H. Mechanistic Studies of the Pyrene-Sensitized Photodecomposition of N-Phenylglycine: Acceleration of the Photodecomposition by the Addition of an Electron Acceptor. *Bull. Chem. Soc. Jpn.* **2000**, *73*, 2783.

(29) Ikeda, S.; Murata, S.; Ishii, K.; Hamaguchi, H. Remarkable Effect of Electron Acceptors on Pyrene-Sensitized Decomposition of N-Phenylglycine. *Chem. Lett.* **1999**, 1009.

(30) Gallagher, S.; Hatoum, F.; Zientek, N.; Oelgemoller, M. Photodecarboxylative Additions of N-Protected Alpha-Amino Acids to N-Methylphthalimide. *Tetrahedron Lett.* **2010**, *51*, 3639.

(31) Hug, G. L.; Bonifačić, M.; Asmus, K.-D.; Armstrong, D. A. Fast Decarboxylation of Aliphatic Amino Acids Induced by 4-Carboxybenzophenone Triplets in Aqueous Solutions. A Nanosecond Laser Flash Photolysis Study. *J. Phys. Chem. B* **2000**, *104*, 6674.

(32) Miyake, Y.; Nakajima, K.; Nishibayashi, Y. Visible Light-Mediated Oxidative Decarboxylation of Arylacetic Acids into Benzyl Radicals: Addition to Electron-Deficient Alkenes by Using Photoredox Catalysts. *Chem. Commun.* **2013**, *49*, 7854.

(33) Miyake, Y.; Nakajima, K.; Nishibayashi, Y. Visible-Light-Mediated Utilization of α-Aminoalkyl Radicals: Addition to

DOI: 10.1021/acs.jpca.6b01141
J. Phys. Chem. A 2016, 120, 2797−2807

Electron-Deficient Alkenes Using Photoredox Catalysts. *J. Am. Chem. Soc.* **2012**, *134*, 3338.
(34) Su, Z. Y.; Mariano, P. S.; Falvey, D. E.; Yoon, U. C.; Oh, S. W. Dynamics of Anilinium Radical α-Heterolytic Fragmentation Processes. Electrofugal Group, Substituent, and Medium Effects on Desilylation, Decarboxylation, and Retro-Aldol Cleavage Pathways. *J. Am. Chem. Soc.* **1998**, *120*, 10676.
(35) Hug, G. L.; Bonifačić, M.; Asmus, K. D.; Armstrong, D. A. Fast Decarboxylation of Aliphatic Amino Acids Induced by 4-Carboxybenzophenone Triplets in Aqueous Solutions. A Nanosecond Laser Flash Photolysis Study. *J. Phys. Chem. B* **2000**, *104*, 6674.
(36) Bonifačić, M.; Stefanic, I.; Hug, G. L.; Armstrong, D. A.; Asmus, K.-D. Glycine Decarboxylation: The Free Radical Mechanism. *J. Am. Chem. Soc.* **1998**, *120*, 9930.
(37) Lalevée, J.; Graff, B.; Allonas, X.; Fouassier, J. P. Aminoalkyl Radicals: Direct Observation and Reactivity toward Oxygen, 2,2,6,6-Tetramethylpiperidine-N-Oxyl, and Methyl Acrylate. *J. Phys. Chem. A* **2007**, *111*, 6991.
(38) Canle, M.; Santaballa, J. A.; Steenken, S. Photo- and Radiation-Chemical Generation and Thermodynamic Properties of the Aminium and Aminyl Radicals Derived from N-Phenylglycine and (N-Chloro,N-Phenyl)Glycine in Aqueous Solution: Evidence for a New Photoionization Mechanism for Aromatic Amines. *Chem. - Eur. J.* **1999**, *5*, 1192.
(39) Merenyi, G.; Lind, J.; Shen, X. Electron Transfer from Indoles, Phenol, and Sulfite (SO_3^{2-}) to Chlorine Dioxide (ClO•). *J. Phys. Chem.* **1988**, *92*, 134.
(40) Solar, S.; Getoff, N.; Surdhar, P. S.; Armstrong, D. A.; Singh, A. Oxidation of Tryptophan and N-Methylindole by N_3•, $Br_2^{\bullet-}$, and $(SCN)_2^{\bullet-}$ Radicals in Light- and Heavy-Water Solutions: A Pulse Radiolysis Study. *J. Phys. Chem.* **1991**, *95*, 3639.
(41) DeFelippis, M. R.; Murthy, C. P.; Faraggi, M.; Klapper, M. H. Pulse Radiolytic Measurement of Redox Potentials: The Tyrosine and Tryptophan Radicals. *Biochemistry* **1989**, *28*, 4847.
(42) Bryant, F. D.; Santus, R.; Grossweiner, L. I. Laser Flash Photolysis of Aqueous Tryptophan. *J. Phys. Chem.* **1975**, *79*, 2711.
(43) Zhu, H.; Wang, W.; Yao, S. Studies on Reaction of Amino Acids and Triplet Thioxanthone Derivatives by Laser Flash Photolysis. *Invest. New Drugs* **2006**, *24*, 465.
(44) Tang, R.; Zhang, P.; Li, H.; Liu, Y.; Wang, W. Photosensitized Oxidation of Tryptophan and Tyrosine by Aromatic Ketones: A Laser Flash Photolysis Study. *Sci. China: Chem.* **2012**, *55*, 386.
(45) Tsentalovich, Y. P.; Morozova, O. B.; Yurkovskaya, A. V.; Hore, P. J. Kinetics and Mechanism of the Photochemical Reaction of 2,2′-Dipyridyl with Tryptophan in Water: Time-Resolved CIDNP and Laser Flash Photolysis Study. *J. Phys. Chem. A* **1999**, *103*, 5362.
(46) Baugher, J. F.; Grossweiner, L. I. Photolysis Mechanism of Aqueous Tryptophan. *J. Phys. Chem.* **1977**, *81*, 1349.
(47) de Lucas, N. C.; Ruis, C. P.; Teixeira, R. I.; Marcal, L. L.; Garden, S. J.; Correa, R. J.; Ferreira, S.; Netto-Ferreira, J. C.; Ferreira, V. F. Photosensitizing Properties of Triplet Furano and Pyrano-1,2-Naphthoquinones. *J. Photochem. Photobiol., A* **2014**, *276*, 16.
(48) Rappon, M.; Syvitski, R. T. Kinetics of Photobleaching of Aberchrome 540 in Various Solvents: Solvent Effects. *J. Photochem. Photobiol., A* **1996**, *94*, 243.
(49) Liu, W. Z.; Bordwell, F. G. Gas-Phase and Solution-Phase Homolytic Bond Dissociation Energies of H-N Bonds in the Conjugate Acids of Nitrogen Bases. *J. Org. Chem.* **1996**, *61*, 4778.
(50) Balakrishnan, G.; Keszthelyi, T.; Wilbrandt, R.; Zwier, J. M.; Brouwer, A. M.; Buma, W. J. The Radical Cation and Lowest Rydberg States of 1,4-Diaza[2.2.2]Bicyclooctane (Dabco). *J. Phys. Chem. A* **2000**, *104*, 1834.
(51) Halpern, A. M.; Forsyth, D. A.; Nosowitz, M. Flash Photolysis of Saturated Amines in Acetonitrile Solution at 248 Nm: Formation of Radical Cations. *J. Phys. Chem.* **1986**, *90*, 2677.
(52) Dunn, D. A.; Schuster, D. I.; Bonneau, R. Photochemistry of Ketones in Solution. 74. Characterization of Transient Intermediates on Laser Flash Excitation of Cyclohexenones in the Presence of Amines. *J. Am. Chem. Soc.* **1985**, *107*, 2802.
(53) De la Fuente, J. R.; Neira, V.; Saitz, C.; Jullian, C.; Sobarzo-Sanchez, E. Photoreduction of Oxoisoaporphine Dyes by Amines: Transient-Absorption and Semiempirical Quantum-Chemical Studies. *J. Phys. Chem. A* **2005**, *109*, 5897.
(54) De la Fuente, J. R.; Aliaga, C.; Poblete, C.; Zapata, G.; Jullian, C.; Saitz, C.; Cañete, A.; Kciuk, G.; Sobarzo-Sanchez, E.; Bobrowski, K. Photoreduction of Oxoisoaporphines by Amines: Laser Flash Photolysis, Pulse Radiolysis and TD-DFT Studies. *J. Phys. Chem. A* **2009**, *113*, 7737.
(55) Demeter, A.; Horváth, K.; Böőr, K.; Molnár, L.; Soós, T.; Lendvay, G. Substituent Effect on the Photoreduction Kinetics of Benzophenone. *J. Phys. Chem. A* **2013**, *117*, 10196.
(56) Boilet, L.; Burdzinski, G.; Buntinx, G.; Lefumeux, C.; Poizat, O. Picosecond Absorption and Resonance Raman Investigation of the Dynamics of the Photoreduction of 4,4′-Bipyridine by Aliphatic Amines in Acetonitrile Solution. *J. Phys. Chem. A* **2001**, *105*, 10271.
(57) Poizat, O.; Buntinx, G.; Boilet, L. Photoreduction of 4,4′-Bipyridine by Amines in Acetonitrile−Water Mixtures: Influence of H-Bonding on the Ion-Pair Structure and Dynamics. *J. Phys. Chem. A* **2005**, *109*, 10813.
(58) Aliaga, C.; Cerón-Neculpán, M.; Saitz, C.; Jullian, C.; Sobarzo-Sánchez, E.; De la Fuente, J. R. Oxoisoaporphines: Regioselective Deuterium Labelling Involving the Metastable Hydrogenated Photoproduct Anions. *J. Photochem. Photobiol., A* **2011**, *222*, 360.
(59) Bent, D. V.; Hayon, E. Excited State Chemistry of Aromatic Amino Acids and Related Peptides. Iii. Tryptophan. *J. Am. Chem. Soc.* **1975**, *97*, 2612.
(60) de Lucas, N. C.; Ruis, C. P.; Teixeira, R. I.; Marçal, L. L.; Garden, S. J.; Corrêa, R. J.; Ferreira, S.; Netto-Ferreira, J. C.; Ferreira, V. F. Photosensitizing Properties of Triplet Furano and Pyrano-1,2-Naphthoquinones. *J. Photochem. Photobiol., A* **2014**, *276*, 16.
(61) Tsentalovich, Y. P.; Snytnikova, O. A.; Sagdeev, R. Z. Properties of Excited States of Aqueous Tryptophan. *J. Photochem. Photobiol., A* **2004**, *162*, 371.
(62) Yadav, P.; Selvaraj, B. T.; Bender, F. L. P.; Behringer, M.; Moradi, M.; Sivadasan, R.; Dombert, B.; Blum, R.; Asan, E.; Sauer, M.; Julien, J.-P.; Sendtner, M. Neurofilament Depletion Improves Microtubule Dynamics Via Modulation of Stat3/Stathmin Signaling. *Acta Neuropathol.* **2016**, DOI: 10.1007/s00401-016-1564-y.
(63) Falini, B.; Albiero, E.; Bolli, N.; De Marco, M. F.; Madeo, D.; Martelli, M.; Nicoletti, I.; Rodeghiero, F. Aberrant Cytoplasmic Expression of C-Terminal-Truncated Npm Leukaemic Mutant Is Dictated by Tryptophans Loss and a New Nes Motif. *Leukemia* **2007**, *21*, 2052.
(64) Horn, S.; Meyer, J.; Heukeshoven, J.; Fehse, B.; Schulze, C.; Li, S.; Frey, J.; Poll, S.; Stocking, C.; Jucker, M. The Inositol 5-Phosphatase Ship Is Expressed as 145 and 135 Kda Proteins in Blood and Bone Marrow Cells in Vivo, Whereas Carboxyl-Truncated Forms of Ship Are Generated by Proteolytic Cleavage in Vitro. *Leukemia* **2001**, *15*, 112.
(65) Musumeci, M. A.; Botti, H.; Buschiazzo, A.; Ceccarelli, E. A. Swapping Fad Binding Motifs between Plastidic and Bacterial Ferredoxin-Nadp(H) Reductases. *Biochemistry* **2011**, *50*, 2111.
(66) Stayton, P. S.; Sligar, S. G. Structural Microheterogeneity of a Tryptophan Residue Required for Efficient Biological Electron Transfer between Putidaredoxin and Cytochrome P-450cam. *Biochemistry* **1991**, *30*, 1845.
(67) Skoging, U.; Liljestrom, P. Role of the C-Terminal Tryptophan Residue for the Structure-Function of the Alphavirus Capsid Protein. *J. Mol. Biol.* **1998**, *279*, 865.

NOTE ADDED AFTER ASAP PUBLICATION

This paper published ASAP on April 26, 2016, with an error in Scheme 1. The corrected version was reposted on April 27, 2016.

DOI: 10.1021/acs.jpca.6b01141
J. Phys. Chem. A 2016, 120, 2797−2807